Nanomedicine

DOI: 10.1002/anie.201100875

Micelle-Based Brain-Targeted Drug Delivery Enabled by a Nicotine Acetylcholine Receptor Ligand**

Changyou Zhan, Bian Li, Luojuan Hu, Xiaoli Wei, Linyin Feng, Wei Fu, and Weiyue Lu**

The blood–brain barrier (BBB) is the key challenge in the development of drugs for diseases of the central nervous system (CNS). The BBB prevents drugs or drug delivery systems from reaching the site of disease because of tight junctions and lack of fenestration.[1] To circumvent this problem, the receptors that are highly expressed on the capillary endothelium of the brain, such as nicotine acetylcholine receptors (nAChRs), have been exploited to facilitate BBB crossing and intracranial transport of drug delivery systems.[2] nAChRs are ligand-gated ion channels that are expressed mainly at the neuromuscular junction of the CNS, including the brain capillary endothelial cells.[3] The extensive expression of nAChRs in the brain and susceptibility to the inhibition by peptide neurotoxins and neurotropic viral proteins endow them with the ability to mediate peptide-based transvascular delivery of various therapeutic agents to the brain.[2d,4] Herein, we report the design of a 16-residue peptide, derived from the loop II region of the snake neurotoxin candoxin, that binds to nAChRs with high affinity. This peptide, termed CDX, enabled drug delivery to the brain when conjugated to paclitaxel-loaded micelles. As a result, tumor growth in intracranial glioblastoma bearing mice was inhibited and their survival was prolonged.

Snake neurotoxins are members of the "three-finger toxin" superfamily characterized by three adjacent loops arranged in a flat, leaflike structure.[5] These toxins are known to bind through the second loop to nAChRs with high affinity and selectivity.[6] Candoxin from the Malayan krait *Bungarus candidus* consists of a single polypeptide chain of 66 amino acid residues with five disulfide bridges, and antagonizes α7 neuronal nAChRs in nanomolar concentrations with poor reversibility.[7] As was shown previously by western blot analysis,[3d] and confirmed by using immunocytochemical staining (Figure S8 in the Supporting Information), the α7 neuronal nAChR is richly expressed in primary brain capillary endothelial cells, and is thus ideally suited for candoxin-mediated, brain-targeted drug delivery. For this study, we designed and evaluated three short peptides derived from the loop II region of candoxin, FKESWREARGTRIERG (CDX), SWREARGTRI (Pocket_CDX), and disulfide bridged CFKESWREARGTRIERGC (Cyclo_CDX).

To investigate whether or not the candoxin-derived peptides are capable of interacting with rat neuronal nAChRs, we performed a competitive binding assay where different concentrations of peptide competed for receptor binding with radiolabeled ^{125}I-α-bungarotoxin, which is a potent antagonist of α7 neuronal nAChRs.[8] All three peptides functioned as competitive antagonists of neuronal nAChRs in a dose-dependent manner (Figure S2). CDX displayed a K_i value of 0.187 μM, which is approximately 20–40 times lower than those of Pocket_CDX and Cyclo_CDX (Table 1). Not surprisingly, CDX is substantially less potent than candoxin in nAChRs binding. The difference in potency is likely attributable, at least in part, to a loss of entropy for CDX, as it is unstructured in aqueous solution, as indicated by circular dichroism spectroscopic analysis (Figure S3).

Table 1: Experimentally determined versus predicted free energies of binding of all synthetic peptides with α7 neuronal nAChR ($\Delta G = 1.3636 \log K_i$).

Peptide	K_i [μM]	Experimental ΔG [kcal mol^{-1}]	Estimated ΔG [kcal mol^{-1}]
CDX	0.187	−9.17	−9.59
Pocket_CDX	4.60	−7.28	−8.17
Cyclo_CDX	7.11	−7.02	−7.85

Based on the structure of candoxin (PDB code: 1JGK) elucidated by NMR spectroscopy, and the crystal structure of acetylcholine-binding protein (AChBP; PDB code: 1YI5) that shares a high degree of sequence identity with the extracellular ligand-binding domain of α7 neuronal nAChRs, we conducted molecular modeling and docking studies to better understand the interactions of the α7 nAChR with the CDX peptides. All three peptides adopt hairpinlike conformations that feature a unique electrostatic potential with segregating cationic and anionic patches (Figure S5,S6). The highly charged tip of CDX penetrates deeply into the hydrophobic binding pocket formed by two adjacent subunits of the α7 nAChR, and the binding is dominated by cation–π

[*] Dr. C. Zhan,[+] B. Li,[+] Dr. X. Wei, Dr. W. Fu, Prof. W. Lu
School of Pharmacy & Key Laboratory of Smart Drug Delivery
Ministry of Education & PLA, Fudan University
Shanghai 201203 (P.R. China)
Fax: (+86) 21-5198-0090
E-mail: weifuuh@gmail.com
wylu@shmu.edu.cn
Dr. L. Hu, Prof. L. Feng
State Key Laboratory of Drug Research
Shanghai Institute of Materia Medica
Shanghai 201203 (P.R. China)
[+] These authors contributed equally to this work.

[**] This work was supported by National Basic Research Program of China (973 Program) 2007CB935800 and 2010CB934000, the "Key New Drug Creation Program" 2009ZX09310-006, and Shanghai Nanotechnology Program (0953nm03300).
Supporting information for this article is available on the WWW under http://dx.doi.org/10.1002/anie.201100875.

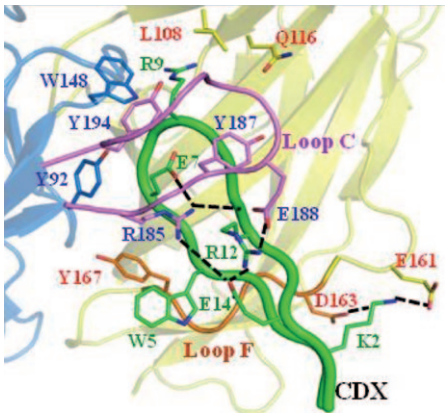

Figure 1. Modeled interactions of CDX with the α7 nAChR. The principal (+) subunit of the receptor is shown in blue and the complementary (−) subunit in yellow. The functionally important loop C is shown in purple and loop F in orange. CDX is depicted as a green wormlike structure. Residues involved in binding are represented by sticks, and hydrogen-bond networks are denoted by black dashed lines.

and electrostatic interactions (Figure 1). Similar modes of binding were observed with Pocket_CDX and Cyclo_CDX (Figure S7), although truncation or cyclization of CDX necessarily altered critical subsite interactions seen with CDX and contributed to a pronounced decrease in binding affinity for the receptor. The contact residues identified by our docking simulation were experimentally demonstrated to be important for the binding of three-finger toxins to the α7 nAChR or its homologues.[9] Importantly, the binding affinities of all three peptides calculated for the α7 nAChR by X-Score[10] are in good agreement with the experimentally determined K_i values (Table 1), thus computationally validating the design of these candoxin-derived peptides as functional antagonists of the α7 nAChR.

To demonstrate the interaction of CDX with the neuronal nAChR receptor in vitro, we incubated biotinylated CDX with primary rat brain capillary endothelial cells, followed by fluorescent staining with fluorescein isothiocyanate (FITC) labeled avidin. An equal molar concentration of biotin was used as a negative control. The fluorescence microscopic images shown in Figure 2 clearly exhibit a specific binding of the cell surface receptors by CDX; this binding is entirely consistent with the immunocytochemical staining and competitive binding data.

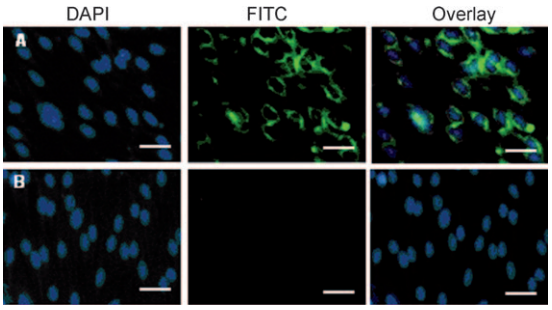

Figure 2. Fluorescently stained CDX bound to primary rat brain capillary endothelial cells. 10 μM of biotinylated CDX (A) or biotin (B) was incubated with fixed cells at 4 °C overnight before adding FITC-conjugated avidin for visualization. Scale bars: 50 μm.

To examine the efficiency of CDX in facilitating nAChR-mediated drug delivery to the brain, we functionalized a polymeric micelle-based delivery vehicle made up of biodegradable poly(ethylene glycol)-poly(D,L-lactide) (PEG–PLA) with CDX. The PEG–PLA micelle, which is a self-assembled nanoparticulate carrier that features a hydrophilic shell and a high-capacity, cargo-loading hydrophobic core, is widely used for the systemic delivery of various hydrophobic drugs and imaging probes.[11] The CDX–PEG–PLA micelle is spherical with a mean diameter of 39 nm, as analyzed by dynamic light scattering and atomic force microscopic techniques (Figure S10). For comparative pharmacokinetic studies, we injected normal KM mice with CDX-decorated and unmodified micelles that encapsulate the fluorescent dye coumarin 6, and chromatographically measured the time-dependent coumarin concentrations in the blood and brain. While functionalization of micelles by CDX had little impact on the pharmacokinetics of coumarin in the blood, CDX decoration of micelles significantly improved the bioavailability of coumarin in the brain as evidenced by an increase of 100% in AUC (area under the curve) (Table S1). These in vivo data suggest that CDX is capable of enhancing drug transport to the CNS.

To further evaluate the potential therapeutic value of CDX-conjugated drug delivery systems, we studied therapeutic efficacy of paclitaxel-loaded CDX–PEG–PLA micelles in a xenograft mouse model of human glioblastoma multiforme (GBM). We intravenously injected three randomly divided groups of nude mice bearing intracranial U87 glioblastoma ($n = 6$) with paclitaxel-encapsulated CDX–PEG–PLA micelles, drug-loaded, unmodified mPEG–PLA micelles, and saline, respectively. As shown in Figure 3, in the absence of CDX, treatment by paclitaxel at a dose of 10 mg per kg of body weight (at 5, 10, and 15 days post-tumor implantation) did little in improving mouse survival, registering a median survival of 20 days versus 19 days for the untreated (saline) group. In contrast, in the presence of CDX, paclitaxel treatment significantly prolonged the average survival time to 27 days ($p < 0.01$, log-rank analysis). In a separate in vivo

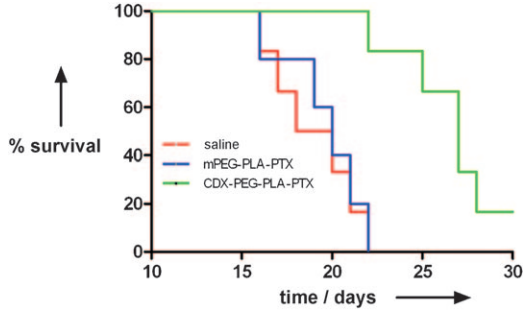

Figure 3. Kaplan–Meier survival curves of nude mice bearing intracranial U87 glioblastoma. Mice that received three doses (at 5, 10 and 15 days post glioblastoma implantation) of CDX–PEG–PLA–PTX micelles survive significantly longer than the control groups that received mPEG–PLA–PTX micelles or physiological saline ($P < 0.01$, log-rank analysis).

study, we treated two groups of U87 tumor-bearing nude mice ($n = 10$) using a different regimen—a lower dose of paclitaxel at 6 mg kg^{-1} injected at 4, 8, 12, and 16 days post-tumor implantation. The group that received CDX-decorated, drug-loaded micelles survived an average of 25.5 days (Figure S11), which is significantly longer than the median survival of 21.5 days for the untreated (saline) group ($p < 0.01$, log-rank analysis). Collectively, these survival data suggest that CDX, when conjugated to a delivery vehicle, can enhance the therapeutic efficacy of traditional chemotherapy drugs for brain tumors.

nAChRs-mediated, improved drug transport to the brain is likely responsible for the enhanced therapeutic efficacy of paclitaxel in the treatment of glioblastoma. To better understand the mechanisms by which CDX–PEG–PLA micelles work in vivo, we analyzed the biodistribution of CDX–PEG–PLA and mPEG–PLA micelles in intracranial U87 glioblastoma-bearing nude mice by using an encapsulated near-infrared fluorescent dye DiR as an indicator. As shown in Figure 4A, caudal vein injection of unmodified mPEG–PLA micelles at 5 days post-glioblastoma implantation resulted in

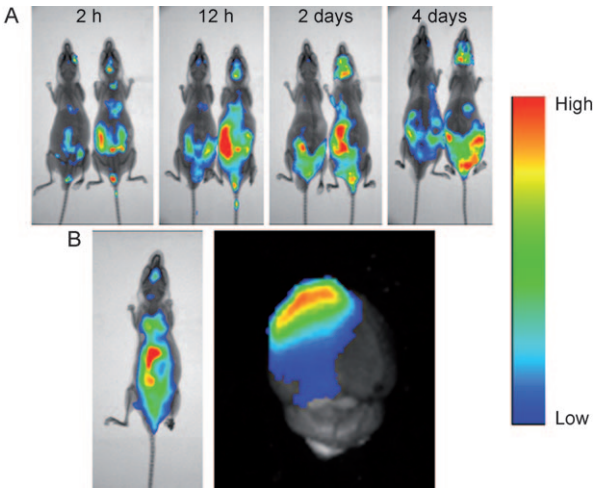

Figure 4. Near-infrared optical images of DiR encapsulated micelles injected in the caudal vein of intracranial glioblastoma-bearing nude mice at 5 days (A) and 15 days (B) post-tumor implantation. The mice on the left-hand side in four pairwise comparisons in panel (A) were injected with DiR-encapsulated mPEG–PLA micelles, and the mice on the right-hand side were injected with CDX–PEG–PLA micelles loaded with the same dose of DiR. The mouse in panel B was sacrificed 12 h after injection of DiR-encapsulated CDX–PEG–PLA micelles, and the brain dissected for imaging.

no accumulation of DiR in the brain over a period of 4 days (2 h, 12 h, 2 days, 4 days). In contrast, pronounced dye accumulation in the brain at each time point was evident with injection of CDX-PEG-PLA micelles. These data indicate that while unmodified mPEG-PLA micelles failed to cross the BBB, CDX functionalization helped breach the barrier and facilitated DiR transport to the brain. Interestingly, tumor progression appears to exacerbate the disintegration of the BBB. When DiR-encapsulated CDX–PEG–PLA micelles were introduced at 15 days post-tumor implantation, the dye accumulated to the site of tumor (Figure 4B)—a phenomenon likely attributable to enhanced permeability and retention (EPR) effects seen with nanoparticles and solid tumors at advanced stages.[12] Tumor-progression-dependent EPR effects may also contribute to the marked difference in survival between treatment groups with and without CDX, despite a CDX-instigated, modest improvement in bioavailability as measured in normal mice.

GBM is the most common primary malignant brain tumor where the BBB impedes effective chemotherapy and results in an extremely poor prognosis.[13] Drug delivery systems that efficiently cross the BBB are urgently needed for the treatment of GBM. We have described CDX, which is a candoxin-derived peptide ligand of neuronal nAChRs, as a novel targeting molecule that enables efficient drug delivery to the brain by overcoming the BBB. In vitro and in vivo studies demonstrate the brain-targeting efficiency of CDX and validate its potential value in improving therapeutic efficacy of existing anticancer drugs such as paclitaxel for the treatment of GBM. As nAChRs are widely expressed in the brain, CDX-inspired, micelle-based drug delivery systems may be broadly applicable to therapeutic intervention for other forms of CNS diseases as well.

Experimental Section

Competitive binding assays: The binding affinities of all peptides with neuronal nAChRs were determined by a radiolabeled competition assay following reported protocols.[4a] A more detailed description of the assay conditions is given in the Supporting Information.

Immunofluorescence: After fixing by an iced methanol/acetone solution (1:1, v/v) for 5 min and permeation by 0.2% Triton X-100, primary rat brain capillary endothelial cells were incubated with biotinylated CDX (10 μM) overnight at 4 °C, and then with FITC-avidin (0.5 mg mL^{-1}; dissolved in phosphate-buffered saline (PBS) containing 1% bovine serum albumen (BSA)) for 30 min at room temperature. After that, cells were washed with PBS and examined by fluorescence microscopy (IX51, Olympus, Japan).

Biodistribution of CDX–PEG–PLA micelles: To study the biodistribution of CDX–PEG–PLA micelles, DIR-encapsulated mPEG–PLA or CDX–PEG–PLA micelles (100 μL) were injected into the tail vein of intracranial glioblastoma bearing nude mice at 5 and 15 days post-tumor implantation. The near infrared imaging was conducted using an in vivo imaging system (FX Pro, Kodak, USA) at different time points after injection.

Received: February 3, 2011
Revised: March 31, 2011
Published online: May 3, 2011

Keywords: drug delivery · micelles · nanomedicine · peptides · receptors

[1] a) K. K. Maiti, O. Y. Jeon, W. S. Lee, D. C. Kim, K. T. Kim, T. Takeuchi, S. Futaki, S. K. Chung, *Angew. Chem.* **2006**, *118*, 2973–2978; *Angew. Chem. Int. Ed.* **2006**, *45*, 2907–2912; b) E. Hutchinson, *Nat. Rev. Neurosci.* **2010**, *11*, 789.

[2] a) W. M. Pardridge, *Mol. Interventions* **2003**, *3*, 90–105, 151; b) B. J. Spencer, I. M. Verma, *Proc. Natl. Acad. Sci. USA* **2007**, *104*, 7594–7599; c) N. J. Abbott, L. Ronnback, E. Hansson, *Nat. Rev. Neurosci.* **2006**, *7*, 41–53; d) P. Kumar, H. Wu, J. L.

McBride, K. E. Jung, M. H. Kim, B. L. Davidson, S. K. Lee, P. Shankar, N. Manjunath, *Nature* **2007**, *448*, 39 – 43.

[3] a) J. M. Lindstrom, *Ann. N. Y. Acad. Sci.* **2003**, *998*, 41 – 52; b) C. Gotti, F. Clementi, *Prog. Neurobiol.* **2004**, *74*, 363 – 396; c) R. C. Hogg, M. Raggenbass, D. Bertrand, *Rev. Physiol. Biochem. Pharmacol.* **2003**, *147*, 1 – 46; d) T. J. Abbruscato, S. P. Lopez, K. S. Mark, B. T. Hawkins, T. P. Davis, *J. Pharm. Sci.* **2002**, *91*, 2525 – 2538.

[4] a) C. Zhan, Z. Yan, C. Xie, W. Lu, *Mol. Pharm.* **2010**, *7*, 1940 – 1947; b) Y. Liu, R. Huang, L. Han, W. Ke, K. Shao, L. Ye, J. Lou, C. Jiang, *Biomaterials* **2009**, *30*, 4195 – 4202.

[5] a) D. Tsernoglou, G. A. Petsko, R. A. Hudson, *Mol. Pharmacol.* **1978**, *14*, 710 – 716; b) V. J. Basus, G. Song, E. Hawrot, *Biochemistry* **1993**, *32*, 12290 – 12298; c) X. Lou, Q. Liu, X. Tu, J. Wang, M. Teng, L. Niu, D. J. Schuller, Q. Huang, Q. Hao, *J. Biol. Chem.* **2004**, *279*, 39094 – 39104; d) G. Polz-Tejera, J. Schmidt, H. J. Karten, *Nature* **1975**, *258*, 349 – 351.

[6] a) A. Roy, X. Zhou, M. Z. Chong, D. D'Hoedt, C. S. Foo, N. Rajagopalan, S. Nirthanan, D. Bertrand, J. Sivaraman, R. M. Kini, *J. Biol. Chem.* **2010**, *285*, 8302 – 8315; b) R. E. Hibbs, G. Sulzenbacher, J. Shi, T. T. Talley, S. Conrod, W. R. Kem, P. Taylor, P. Marchot, Y. Bourne, *EMBO J.* **2009**, *28*, 3040 – 3051; c) T. L. Lentz, P. T. Wilson, E. Hawrot, D. W. Speicher, *Science* **1984**, *226*, 847 – 848; d) T. L. Lentz, E. Hawrot, P. T. Wilson, *Proteins Struct. Funct. Genet.* **1987**, *2*, 298 – 307.

[7] a) S. Nirthanan, E. Charpantier, P. Gopalakrishnakone, M. C. Gwee, H. E. Khoo, L. S. Cheah, D. Bertrand, R. M. Kini, *J. Biol. Chem.* **2002**, *277*, 17811 – 17820; b) S. Nirthanan, E. Charpantier, P. Gopalakrishnakone, M. C. Gwee, H. E. Khoo, L. S. Cheah, R. M. Kini, D. Bertrand, *Br. J. Pharmacol.* **2003**, *139*, 832 – 844.

[8] a) I. W. Jones, J. Barik, M. J. O'Neill, S. Wonnacott, *J. Neurosci. Methods* **2004**, *134*, 65 – 74; b) J. L. Eiselé, S. Bertrand, J. L. Galzi, A. Devillers-Thiery, J. P. Changeux, D. Bertrand, *Nature* **1993**, *366*, 479 – 483.

[9] a) K. Brejc, W. J. van Dijk, R. V. Klaassen, M. Schuurmans, J. van Der Oost, A. B. Smit, T. K. Sixma, *Nature* **2001**, *411*, 269 – 276; b) Y. Bourne, T. T. Talley, S. B. Hansen, P. Taylor, P. Marchot, *EMBO J.* **2005**, *24*, 1512 – 1522; c) P. H. Celie, I. E. Kasheverov, D. Y. Mordvintsev, R. C. Hogg, P. van Nierop, R. van Elk, S. E. van Rossum-Fikkert, M. N. Zhmak, D. Bertrand, V. Tsetlin, T. K. Sixma, A. B. Smit, *Nat. Struct. Mol. Biol.* **2005**, *12*, 582 – 588.

[10] R. Wang, L. Lai, S. Wang, *J. Comput.-Aided Mol. Des.* **2002**, *16*, 11 – 26.

[11] a) K. Yasugi, Y. Nagasaki, M. Kato, K. Kataoka, *J. Controlled Release* **1999**, *62*, 89 – 100; b) N. Nasongkla, E. Bey, J. Ren, H. Ai, C. Khemtong, J. S. Guthi, S. F. Chin, A. D. Sherry, D. A. Boothman, J. Gao, *Nano Lett.* **2006**, *6*, 2427 – 2430; c) N. Kang, M. E. Perron, R. E. Prud'homme, Y. Zhang, G. Gaucher, J. C. Leroux, *Nano Lett.* **2005**, *5*, 315 – 319.

[12] a) J. J. Verhoeff, O. van Tellingen, A. Claes, L. J. Stalpers, M. E. van Linde, D. J. Richel, W. P. Leenders, W. R. van Furth, *BMC Cancer* **2009**, *9*, 444; b) J. R. Ewing, S. L. Brown, M. Lu, S. Panda, G. Ding, R. A. Knight, Y. Cao, Q. Jiang, T. N. Nagaraja, J. L. Churchman, J. D. Fenstermacher, *J. Cereb. Blood Flow Metab.* **2006**, *26*, 310 – 320; c) L. L. Muldoon, C. Soussain, K. Jahnke, C. Johanson, T. Siegal, Q. R. Smith, W. A. Hall, K. Hynynen, P. D. Senter, D. M. Peereboom, E. A. Neuwelt, *J. Clin. Oncol.* **2007**, *25*, 2295 – 2305.

[13] a) C. Zhan, B. Gu, C. Xie, J. Li, Y. Liu, W. Lu, *J. Controlled Release* **2010**, *143*, 136 – 142; b) V. Laquintana, A. Trapani, N. Denora, F. Wang, J. M. Gallo, G. Trapani, *Expert Opin. Drug Delivery* **2009**, *6*, 1017 – 1032; c) F. I. Staquicini, M. G. Ozawa, C. A. Moya, W. H. Driessen, E. M. Barbu, H. Nishimori, S. Soghomonyan, L. G. Flores 2nd, X. Liang, V. Paolillo, M. M. Alauddin, J. P. Basilion, F. B. Furnari, O. Bogler, F. F. Lang, K. D. Aldape, G. N. Fuller, M. Hook, J. G. Gelovani, R. L. Sidman, W. K. Cavenee, R. Pasqualini, W. Arap, *J. Clin. Invest.* **2011**, *121*, 161 – 173.

